Spectrum of Wind Power Fluctuations

M. M. Bandi*
Collective Interactions Unit, OIST Graduate University, Okinawa 904-0495, Japan
(Received 15 September 2016; published 13 January 2017)

Wind power fluctuations for an individual turbine and plant have been widely reported to follow the Kolmogorov spectrum of atmospheric turbulence; both vary with a fluctuation time scale τ as $\tau^{2/3}$. Yet, this scaling has not been explained through turbulence theory. Using turbines as probes of turbulence, we show the $\tau^{2/3}$ scaling results from a large scale influence of atmospheric turbulence. Owing to this long-range influence spanning 100s of kilometers, when power from geographically distributed wind plants is summed into aggregate power at the grid, fluctuations average (geographic smoothing) and their scaling steepens from $\tau^{2/3} \to \tau^{4/3}$, beyond which further smoothing is not possible. Our analysis demonstrates grids have already reached this $\tau^{4/3}$ spectral limit to geographic smoothing.

DOI: 10.1103/PhysRevLett.118.028301

All renewables fluctuate with the natural variability in their energy sources [1,2]. Wind [3] and solar photovoltaics [4], in particular, exhibit fluctuations over a range of magnitudes and time scales (from milliseconds up to a day). Such fluctuations threaten electrical grid stability [5,6] when their magnitudes form a large fraction of power carried by the grid over time scales comparable to the grid response time. Consequently, grid integrity demands increased ancillary reserves, in turn adding to the cost of renewables [7]. In addition, dynamically balancing the ever present consumer load fluctuations with the variable power output of renewables becomes very challenging [8]. Naturally, understanding fluctuations in renewables is of great import in designing strategies to mitigate or manage their fluctuations. Increasing penetration of renewables within the global energy mix also renders this problem very timely and relevant.

The power generated by a wind turbine fluctuates with varying wind speed and indeed, its spectrum is widely believed to reflect the Kolmogorov spectrum [9] of atmospheric turbulence; both vary with frequency f as $f^{-5/3}$ [10–12] or with time scale τ as $\tau^{2/3}$ [13]. This variability decreases when fluctuations are averaged in the aggregate power feeding the grid from geographically distributed wind plants [14], a mechanism referred to as *geographic smoothing*. Despite costs associated with variability [15], neither the $\tau^{2/3}$ fluctuation scaling nor the geographic smoothing mechanism are understood.

We provide a minimal description of the wind power fluctuation spectrum from the turbine through grid scales from a turbulence theory standpoint and experimentally verify it with wind plant data. The $\tau^{2/3}$ wind power fluctuation scaling results from the largest length scales of atmospheric turbulence spanning hundreds of kilometers, influencing the small scales where individual turbines operate. This long-range influence correlates power outputs from geographically distributed plants over a range of time scales that falls with interplant distance. Consequently, aggregate grid-scale power fluctuations smooth until they reach a limiting spectrum with $\tau^{4/3}$ scaling.

The power P generated by a wind turbine relates to wind speed u blowing past the turbine through the power relation $P = (\frac{1}{2})\rho A\gamma u^3$. Here, ρ is air density, A is the turbine rotor cross sectional area, and γ is the turbine efficiency. This dimensional argument can be expressed in time-dependent form as (Supplemental Material [16])

$$P(t) = K[\bar{u}^3 + 3\bar{u}^2\tilde{u}(t) + 3\bar{u}\,\tilde{u}(t)^2 + \tilde{u}(t)^3], \qquad (1)$$

where $K = (\frac{1}{2})\rho A\gamma$, $\bar{u}$ is the time-independent mean, and $\tilde{u}(t)$ is the time-varying fluctuation in speed [$\overline{\tilde{u}(t)} = 0$]. We analyze wind power fluctuations from a turbulence standpoint by treating the turbine as a temporal, Eulerian probe, much like an anemometer, whose output is a function of time-varying turbulent wind speed past a fixed (Eulerian) spatial point (Supplemental Material [16]). Assuming the turbine extracts the same fraction of power at all frequencies, i.e., no dispersion and that the power conversion is adiabatic, characteristics of Eulerian, temporal fluctuations in atmospheric turbulence apply to wind power alike. This idealized assumption fails at time scales $\tau \leq \tau_R$ [11], where $\tau_R \sim$ tens of seconds is the turbine reaction time scale, but holds at long time scales ($\tau_R < \tau < \tau_0$) until velocity fluctuations decorrelate at the large eddy turnover time τ_0 (Table I).

We deduce the second order structure function for wind power in terms of wind speed by substituting Eq. (1) in

TABLE I. Definitions of parameters and variables.

Quantity	Description
l_0	Integral length scale
τ_0	Large eddy turnover time
η	Kolmogorov length scale
$\bar{\varepsilon}$	Mean energy flux per unit mass
$\tilde{u}_{\|\|}(\vec{r})$	Longitudinal velocity at coordinate $\vec{r}$
$\Delta u^m_{\|\|}(r)$	$[\tilde{u}_{\|\|}(\vec{R}+\vec{r})^m - \tilde{u}_{\|\|}(\vec{R})^m]$
$\Delta u^m(\tau)$	$[\tilde{u}(t+\tau)^m - \tilde{u}(t)^m]$
$S^m_n(r)$	$\langle[\Delta u^m_{\|\|}(r)]^n\rangle$
$S^m_n(\tau)$	$\langle[\Delta u^m(\tau)]^n\rangle$
$u_{\rm rms}$	rms velocity $\sqrt{\bar{\tilde{u}}^2} \equiv \sqrt{\langle[\Delta u(\tau_0)]^2\rangle}$.
$\Delta P(\tau)$	$[P(t+\tau) - P(t)]$
$D_2(\tau)$	$\langle[\Delta P(\tau)]^2\rangle$

$\Delta P(\tau)$ (Table I) and computing $D_2(\tau) = \langle\{K[3\bar{u}^2\Delta u^1(\tau) + 3\bar{u}\Delta u^2(\tau) + \Delta u^3(\tau)]\}^2\rangle$, obtaining to leading order (ignoring higher order cross terms)

$$D_2(\tau) \sim 9K^2\bar{u}^4 S^1_2(\tau) + 9K^2\bar{u}^2 S^2_2(\tau) + K^2 S^3_2(\tau). \quad (2)$$

Equation (2) now affords us an interpretation of the wind power fluctuation spectrum through the framework of turbulence theory. We analyzed scalings for all terms in Eq. 2 with data from a 2.05 MW MM92 REPower turbine in Howard, NY. The simultaneous wind speed and power time series sampled at 0.2 Hz for 20 day duration had mean speed $\bar{u} = 8.04\ \mathrm{m\,s^{-1}}$ and rms fluctuation $u_{rms} = 4.58\ \mathrm{m\,s^{-1}}$. Autocorrelation functions [Fig. 1(a)] yielded a large eddy turnover time $\tau_0 = 13$ h for wind speed and decorrelation time of 14 h for power, clearly pointing to the strong influence of diurnal oscillations on signal correlation.

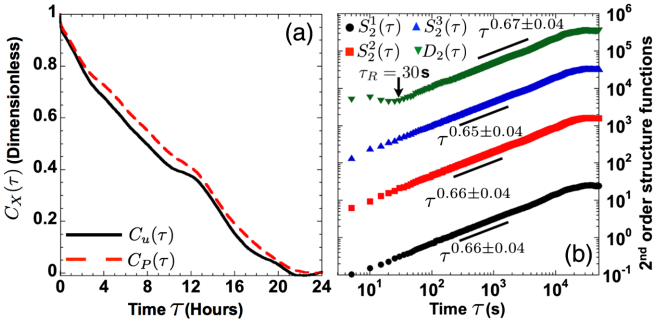

FIG. 1. (a) Autocorrelation functions $[C_X(\tau) = [\overline{X(t)X(t+\tau)}/\overline{X(t)^2}]$, where $X(t) = \tilde{u}(t)$ for wind speed and $P(t) - \bar{P}$ for wind power] exhibit correlation time of $\tau_0 = 13$ h (large eddy turnover time) for wind speed (solid black line) and 14 h for wind power (dashed red line). (b) $S^1_2(\tau)$ (solid black circles), $S^2_2(\tau)$ (solid red squares), $S^3_2(\tau)$ (solid blue triangles) representing rhs and $D_2(\tau)$ (solid green inverted triangles), the lhs of Eq. (2), all scale as $\tau^{2/3}$ within measurement error (± 0.04). $D_2(\tau) \sim \tau^{2/3}$ scaling deviates for $\tau \le \tau_R = 30$ s.

Figure 1(b) plots all terms in Eq. (2) for Howard data. Barring deviations at short time scales ($\tau \le \tau_R \simeq 30$ s) expected from rotor inertia, $D_2(\tau) \sim \tau^{0.67\pm0.04}$ agrees with prior empirical results [10–12]. All $S^m_2(\tau) \sim \tau^{2/3}$ in Eq. (2) to within measurement error, in accord with atmospheric turbulence measurements [35] in the absence of turbines. We now explain this $\tau^{2/3}$ scaling through turbulence theory.

Turbulent kinetic energy is transported in fluid parcels, loosely termed "eddies", of finite spatial extent over which velocity fluctuations are correlated. When transported past a stationary, Eulerian probe, an eddy registers a fluctuation of finite duration. Fluctuations therefore represent the length r and time τ scales within the inertial range of turbulence $\eta < r < l_0$ (Table I). Kolmogorov's 1941 theory (K41) [9] elucidates the velocity ($\tilde{u}^1$) fluctuation spectrum within the inertial range of fully developed (high Reynolds Re) three dimensional turbulence through the second order structure function $S^1_2(r) = C_1(\bar{\varepsilon}r)^{2/3}$ [$C_1 \sim \mathcal{O}(1)$ constant]. Since we are concerned with temporal wind power fluctuations, Taylor's hypothesis (TH) [36] permits a convenient [37] switch from length to time scales $r \equiv \bar{u}\tau$ to retrieve the Eulerian, temporal second order structure function $S^1_2(\tau) = C_1(\bar{u}\,\bar{\varepsilon}\,\tau)^{2/3}$. Whereas K41 concerns only velocity fluctuations $[S^1_2(\tau)]$, Eq. (2) contains additional terms $S^2_2(\tau)$ and $S^3_2(\tau)$.

Dimensional analysis similar to K41 extended to arbitrary powers of velocity yields $S^m_n(r) \sim (\bar{\varepsilon}r)^{2m/3}$ (Supplemental Material [16]), but substituting $r \equiv \bar{u}\tau$ does not convert these expressions from space to time. This conversion depends on the relative magnitude of mean speed to rms fluctuations ($u_{\rm rms}/\bar{u}$). When $u_{\rm rms}/\bar{u} \ll 1$, (operationally $u_{\rm rms}/\bar{u} < 0.1$), the uniform sweeping regime arises where TH applies. Here, eddies do not measurably evolve over measurement duration as they are swept past the Eulerian probe by $\bar{u}$, thus yielding

$$D_2(\tau) \sim 9K^2\bar{u}^{14/3}(\bar{\varepsilon}\tau)^{2/3} + 9K^2\bar{u}^{8/3}u^2_{\rm rms}(\bar{\varepsilon}\tau)^{2/3} + K^2u^4_{\rm rms}(\bar{u}\,\bar{\varepsilon}\,\tau)^{2/3}. \quad (3)$$

$S^2_2(\tau)$ & $S^3_2(\tau)$ scalings differ from K41 dimensional expectations due to breakdown of Galilean invariance (Supplemental Material [16]). When $u_{\rm rms}/\bar{u} > 0.1$, the random sweeping hypothesis (RSH) applies and accounts for eddy evolution over measurement duration, yielding

$$D_2(\tau) \sim 9K^2\bar{u}^4(u_{\rm rms}\bar{\varepsilon}\tau)^{2/3} + 9K^2\bar{u}^2u^{8/3}_{\rm rms}(\bar{\varepsilon}\tau)^{2/3} + K^2u^{14/3}_{\rm rms}(\bar{\varepsilon}\tau)^{2/3}. \quad (4)$$

The left-hand side (lhs) of Eqs. (3) and (4) will exhibit $D_2(\tau) \sim \tau^{2/3}$ scaling over the range of time scales $\tau_R < \tau < \tau_0$. For $\tau \le \tau_R$, $D_2(\tau)$, scaling will deviate due to turbine inertia and control system dynamics, but $S^1_2(\tau)$, $S^2_2(\tau)$, and $S^3_2(\tau)$ scalings on right-hand side (rhs) of

Eqs. (3) and (4) will persist. As $\tau \to \tau_0$, all scalings will deviate from $\tau^{2/3}$ scalings due to loss of correlation. All these features are observed in Fig. 1(b). Whereas $u_{\rm rms}/\bar{u} \simeq 0.57$ places Howard data [Fig. 1(b)] within the RSH regime (Eq. (4)), TH and RSH in fact represent two limits. In reality, both $\bar{u}$ and $u_{\rm rms}$ participate in eddy transport; hence, it requires the application of a combination of TH and RSH [38,39]. Nonetheless, this has no impact on the $\tau^{2/3}$ scaling since both Eqs. (3) and (4) yield the same exponent.

To our knowledge, this is the first physical explanation of the wind turbine power fluctuation spectrum. The presence of $u_{\rm rms}$ in $D_2(\tau)$ implies power fluctuations in an individual turbine contain signatures of the largest scales of atmospheric turbulence. Furthermore, two turbines distance $d \leq l_0$ apart exhibit correlated power fluctuations over a range of time scales that varies with d. This is owing to $u_{\rm rms}$ being the integral scale (l_0) velocity fluctuation, through which the largest scales of atmospheric turbulence exert influence upon individual turbines. An estimate of the integral scale from Howard data yields $l_0 = u_{\rm rms}\tau_0 = 4.58\,{\rm ms}^{-1} \times 13\,{\rm h} = 214\,{\rm km}$, clearly, a consequence of diurnal oscillation time scale dominating over the long signal correlation time (Supplemental Material [16]). This estimate is in good agreement with independent studies that directly measured interplant, instantaneous (zero time lag, $\tau = 0$) power fluctuation correlations which fell with distance. This decay in correlation was fit with an exponential $[e^{(-d/D)}]$ providing a correlation decay length $D\sim$ hundreds of km; $D = 641$ km (Europe) [40], $D = 305$ km (Electric Reliability Council Of Texas ERCOT system, Texas) [14], $D = 375$ km (Germany) [41], and $D = 500$ km (Denmark) [42]. Henceforth, we assume $l_0 \simeq D$ in all subsequent analysis.

We now consider aggregate power fluctuations in a wind plant comprising, say M turbines. If individual turbines were uncorrelated, aggregate plant fluctuations would smooth as $1/\sqrt{M}$, and the spectrum would continually steepen τ^{ζ} (with $\zeta > 2/3$) with increasing M. Such is not the case; wind plant power fluctuations also exhibit $\tau^{2/3}$ scaling [10,12,14]. At least three sources of turbulence must be considered at the plant level—turbulence generated by the atmospheric boundary layer (boundary layer dynamics), collective distortion of flow fields in the vicinity of a plant by turbine wakes (plant generated turbulence) [43,44], and finally, turbulence from the largest length scales of atmospheric flows (atmospheric turbulence). An estimate of τ_0 for the three sources, and its comparison with duration out to which scalings persist, proves useful in determining the dominant source of fluctuations.

Using a representative value of $u_{\rm rms} \sim 4\ {\rm m\,s^{-1}}$ and $l_0 \sim 1$ km for the atmospheric boundary layer thickness [45], we estimate $\tau_0 = l_0/u_{\rm rms} = 250\,{\rm s} \sim 4$ min. Plant generated turbulence would possess an integral scale $l_0 \sim$ few kilometers, the plant's linear dimension. Taking a putative plant linear dimension of 5 km yields a large eddy turnover time estimate of $\tau_0 = 5000\ {\rm m}/4\ {\rm m\,s^{-1}} = 1250\ {\rm s} \sim$tens of minutes. Atmospheric turbulence yields $\tau_0 \sim 10$ h as already estimated from Howard data. Estimates of τ_0 for boundary layer dynamics (few minutes) and plant generated turbulence (tens of minutes) are much shorter than the ~10 h duration up to which $\tau^{2/3}$ scaling persists in aggregate plant power fluctuations [10,14]. In Fig. 2(a), we plot the second order structure function of power fluctuations for a single wind plant ($N = 1$) in the ERCOT system (15 min sampling for 1 yr duration, previously presented in Ref. [14]). There too, we see $\tau^{0.68\pm0.05}$ persists up to $\tau = 11$ h.

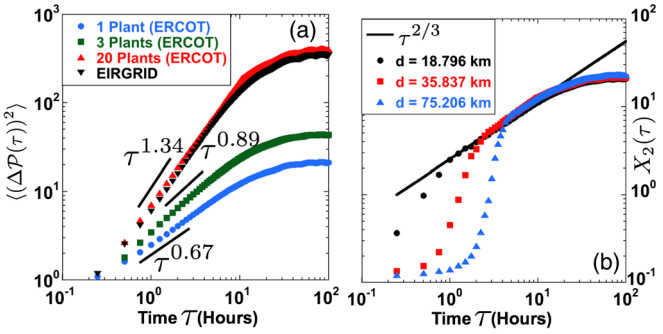

FIG. 2. (a) Aggregate power scaling $\langle[\Delta\mathcal{P}(\tau))]2\rangle = A\tau^{\zeta}$ steepens with increasing number of plants N from $\zeta = 0.68 \pm 0.05$ ($N = 1$, solid blue circles) through $\zeta = 0.89 \pm 0.05$ ($N = 3$, solid green squares) until scaling saturates at $\zeta = 1.39 \pm 0.05$ ($N = 20$, solid red triangles) for ERCOT. EIRGRID data ($N = 224$, solid black inverted triangles) yields $\zeta = 1.34 \pm 0.01$ in exact agreement with $\zeta = 4/3$ bound. (b) $X_2(\tau)$ for interplant distance $d = 18.796$ km (solid black circles), $d = 35.837$ km (solid red squares) and $d = 75.206$ km (solid blue triangles) shows $X_2(\tau) = B\tau^{2/3}$ for $\tau > \tau_d$, where τ_d monotonically increases with d. All curves in (a) and (b) were normalized ($A = B = 1$) for easy comparison.

Irrespective of the turbulent source that generates eddies, it is $\bar{u}$ and $u_{\rm rms}$ of large scale atmospheric flows that transport eddies past the plant [39]. The presence of $u_{\rm rms}$ in the turbine spectrum (Eqs. (3) and (4)) assures plant generated turbulence and boundary layer dynamics are slave to the longer time scale dynamics of large scale atmospheric structures which contain the most energy. Aggregate plant power smooths over short time scales corresponding to fluctuation time scales of eddies of size $r \leq d$, where d is interturbine spacing. However, over $D \sim$ hundreds of km, a plant few kilometers in span behaves as an integral probe for all eddies larger than itself, since these large eddies strongly correlate all turbine outputs. As a result, one observes the $\tau^{2/3}$ spectral scaling extend from the turbine to the plant scale.

Moving from a single ($N = 1$) plant, we now consider grid level fluctuations in aggregate wind power $\mathcal{P}(t) = \Sigma_{i=1}^{N}\Sigma_{j=1}^{M_i}P_{ij}(t)$ from several ($N > 1$) distributed wind plants, each with M_i turbines. In Fig. 2(a), we plot the second order structure function $\langle[\Delta\mathcal{P}(\tau)]^2\rangle \equiv \langle[\mathcal{P}(t+\tau) - \mathcal{P}(t)]^2\rangle$ for composite wind power $\mathcal{P}(t)$ for $N = 1$, 3, and

20 wind plants in the ERCOT system. The scaling $\langle[\Delta\mathcal{P}(\tau)]^2\rangle \sim \tau^{\zeta}$ steepens with increasing N from the expected $\zeta = 0.68 \pm 0.05$ $(N = 1)$ through $\zeta = 0.89 \pm 0.05$ $(N = 3)$ before saturating at $\zeta = 1.39 \pm 0.05$ $(N = 20)$. To emphasize the scaling saturation, we overlay observed scaling for data (15 min sampling over 5 yr) from the Irish grid (EIRGRID) [46] comprising $N = 224$ plants, previously published in Ref. [3], which yields $\zeta = 1.34 \pm 0.01$. Larger the value of ζ (steeper scaling of $\langle[\Delta\mathcal{P}(\tau)]^2\rangle$), greater the geographic smoothing magnitude. The fact that scaling stalls at $\zeta = 4/3$ despite an order of magnitude increase in the number of wind plants from $N = 20$ (ERCOT) to $N = 224$ (EIRGRID) implies, there exists a limit to geographic smoothing.

Large scale atmospheric influence directly impacts geographic smoothing through instantaneous correlations in interplant power outputs. Since large scales convect small eddies nesting within them, two plants distance d apart become correlated by eddies of size $d < r < l_0$ and exhibit correlated power fluctuations in the range of time scales $\tau_d < \tau < \tau_0$ and vanish for $\tau \leq \tau_d$, τ_d being the fluctuation time scale for eddy of size $r \equiv d$. From the above physical picture, we expect the second order cross-structure function of wind power defined as $X_2(\tau) \equiv \langle[P_k(t+\tau) - P_l(t)]^2\rangle$ between plant pairs k and l distance d apart, will scale as $X_2(\tau) \sim \tau^{2/3}$ for $\tau > \tau_d$ and vanish for $\tau \leq \tau_d$. This expectation assumes the two wind plants are collinear along the streamwise direction of large scale flow and would only work if directional fluctuations are small and infrequent. Since ERCOT data did not contain wind direction information, we confirmed collinearity of plant separation with prevalent wind direction using monthly averages from land based stations through the NOAA database [47]. Figure 2(b) shows $X_2(\tau)$ scaling for three representative wind plant pairs in the ERCOT system where this expectation is met. A clear time scale (τ_d) is discernible below which no scaling exists, and above which $X_2(\tau) \sim \tau^{2/3}$ holds. Importantly, τ_d monotonically increases with interplant distance d, thus supporting our expectation.

We now use the above framework to explain the geographic smoothing mechanism and its $\tau^{4/3}$ spectral limit. Consider N distributed wind plants, with interplant distance d less than $(d < D)$, comparable to $(d \simeq D)$, or greater than $(d > D)$ spatial correlation length D $(l_0 \simeq D)$. Summing all outputs into a composite signal $\mathcal{P}(t)$ representing the aggregate grid-scale wind power, we see $\mathcal{P}(t) = \Sigma_{i=1}^{N}\Sigma_{j=1}^{M_i} P_{ij}(t) = K_{ij}[\bar{u_{ij}}^3 + 3\bar{u_{ij}}^2\tilde{u_{ij}}(t) + 3\bar{u_{ij}}\,\tilde{u_{ij}}(t)^2 + \tilde{u_{ij}}(t)^3]$. As odd functions, $\tilde{u_{ij}}(t)$ and $\tilde{u_{ij}}(t)^3$ take positive and negative values at different spatial locations for each instantaneous snapshot, with their sum approaching a small, nonzero value. However, $\tilde{u_{ij}}(t)^2$ being quadratic and always positive is amplified under summation $\Sigma_{i,j}\tilde{u_{ij}}(t)^2$ and exerts control over grid-scale fluctuations. Since the efficacy of geographic smoothing depends upon the decay of spatiotemporal correlations in $\mathcal{P}(t)$, we examine its temporal, two-point correlator given by

$$\mathcal{P}(t)\bar{\mathcal{P}}(t+\tau) = \sum_{k,l} P_k(t)\bar{P_k}(t+\tau) + P_k(t)\bar{P_l}(t+\tau). \quad (5)$$

When individual plant outputs are summed, the cross-correlation term (second term in rhs of Eq. (5) encoding long-range spatial correlations decays with increasing interplant distance and $\Sigma_{k,l}P_k(t)\bar{P_l}(t+\tau) \to 0$ as $d \to D$. This leaves only the self-correlation term $[\Sigma_{k,l}P_k(t)\bar{P_k}(t+\tau)]$, which represents true K41 scalings.

Whereas temporal sampling at an Eulerian point yields a non-Galilean invariant temporal spectrum for wind power, the temporal spectrum of a spatially averaged signal is Galilean invariant by default and respects K41 scalings [38]. Scaling up from $N = 1$ towards several $(N > 1)$ distributed plants spanning an area $\sim D^2$ feeding the grid, one approaches the asymptotic field averaged limit. In this limit, cross-correlations in Eq. (5) decay and the signal self-correlation is retained with true K41 scaling. Whereas the asymptotic convergence would occur as $\sqrt{N}$ if plants were independent, long range spatial correlation permits faster convergence as observed in Fig. 2(a). Consequently, grid-scale aggregate power fluctuations $\langle[\Delta\mathcal{P}(\tau)]^2\rangle$ follow K41 dimensional scaling for $\tilde{u}(\tau)^2$, i.e. $\langle[\Delta\mathcal{P}(\tau)]^2\rangle \sim S_2^2(\tau) \sim \tau^{4/3}$ (Supplemental Material [16]). In fact, since one can never escape self-correlations, grid-scale fluctuations cannot smooth beyond this natural scaling limit; $\langle[\Delta\mathcal{P}(\tau)]^2\rangle \sim \tau^{\zeta}$ will steepen and ζ will increase from $\zeta = 2/3$ for a single plant to $\zeta = 4/3$ at the grid scale and stall there. Further increase in the number of wind plants N cannot smooth fluctuations past this natural spectral bound as clearly evidenced from Fig. 2(a).

In summary, knowledge of the spectral bound and validation of its existence has immediate implications for wind engineering and policy alike. Once the spectral limit is hit, adding power from more plants located within the correlation distance D does not change the spectrum. Adding power from plants situated beyond the correlation length will contribute more power to the zero frequency mode (mean power) and the spectrum will shift down, but will retain its $4/3$ spectral slope. Knowledge of this spectral limit helps estimate the ancillary reserves [48] needed on standby for a grid of given size and response time. The known spectral form, when fed as input to a stochastic load scheduling protocol [49], could potentially alleviate dynamic load balancing challenges. Similar spectral limits, if they exist, for other renewables such as solar [4], could inform policy by helping estimate the optimal energy mix for a regional grid with known set of resource constraints.

This work was supported by the Collective Interactions Unit, OIST Graduate University. M. M. B. thanks J. Apt for ERCOT and Howard data, EIRGRID for Irish data, and

acknowledges discussions with J. Apt, N. Goldenfeld, S. Mandre, B. Fox-Kemper, I. Procaccia, S. Ciliberto, G. Falkovich, M. Chertkov, M. Venkadesan, N. Ouellette, and S. Kurien.

*bandi@oist.jp

[1] D. J. C. MacKay, *Sustainable Energy—Without the Hot Air* (UIT Cambridge Ltd., Cambridge, England, 2009).
[2] J. Apt and P. Jaramillo, *Variable Renewable Energy and the Electricity Grid* (Taylor and Francis, London, 2014).
[3] G. Bel, C. P. Connaughton, M. Toots, and M. M. Bandi, New J. Phys. **18**, 023015 (2016).
[4] K. Klima and J. Apt, Envir. Res. Lett. **10**, 104001 (2015).
[5] R. Wiser, Z. Yang, M. Hand, O. Hohmeyer, D. Infield, P. H. Jensen, V. Nikolaev, M. O'Malley, G. Sinden, and A. Zervos, *Wind Energy, In IPCC Special Report on Renewable Energy Sources and Climate Change Mitigation* (Cambridge University Press, Cambridge, England and New York, USA, 2011).
[6] J. O. G. Tande, Appl. Energy **65**, 395 (2000).
[7] C. Leuken, G. E. Cohen, and J. Apt, Environ. Sci. Technol. **46**, 9761 (2012).
[8] M. A. Matos and R. J. Bessa, IEEE Transactions on Power Systems;IEEE Transactions on Power Electronics **26**, 594 (2011).
[9] A. N. Kolmogorov, Dokl. Akad. Nauk SSSR **30**, 299 (1941) [Sov. Phys. Dokl.].
[10] J. Apt, J. Power Sources **169**, 369 (2007).
[11] P. Milan, M. Wächter, and J. Peinke, Phys. Rev. Lett. **110**, 138701 (2013).
[12] R. Calif, R. Schmitt, and Y. Huang, Physica (Amsterdam) **392A**, 4106 (2013).
[13] Whereas published results we cite are in frequency domain, to maintain consistency with our analysis, we quote all results in the time domain with the understanding that $\tau^{\zeta} \Leftrightarrow f^{-(\zeta+1)}$.
[14] W. Katzenstein, E. Fertig, and J. Apt, Energy Policy **38**, 4400 (2010).
[15] W. Katzenstein and J. Apt, Energy Policy **51**, 233 (2012).
[16] See Supplemental Material at http://link.aps.org/supplemental/10.1103/PhysRevLett.118.028301, for wind turbine power relation, turbine power conversion, K41 dimensional consideration, TH versus RSH and Galilean invariance breakdown, and Integral scale of atmospheric turbulence, which includes Refs. [17–34].
[17] E. Kulunk, in *Fundamental and Advanced Topics in Wind Power,* edited by R. Carriveau (Intech, 2011), Chap. 1.
[18] T. Burton, D. Sharpe, N. Jenkins, and E. Bossanyi, *Wind Energy Handbook* (John Wiley & Sons Ltd., England, 2001).
[19] C. V. Moreno, H. A. Duarte, and J. U. Garcia, IEEE Trans. Energy Convers. **17**, 267 (2002).
[20] A. Choukulkar, Y. Pichugina, C. T. M. Clack, R. Calhoun, R. Banta, A. Brewer, and M. Hardesty, Wind Energ., doi:10.1002/we.1929 (2015).
[21] D. A. Dutton and D. G. Deaven, in *Some Properties of Atmospheric Turbulence. In Statistical Models and Turbulence. Lecture Notes in Physics,* edited by M. Rosenblatt and C. W. Van Atta (Springer, New York, 1972), Vol. 12.
[22] R. H. Kraichnan, Phys. Fluids **7**, 1723 (1964).
[23] H. Tennekes, J. Fluid Mech. **67**, 561 (1975).
[24] S. Chen and R. H. Kraichnan, Phys. Fluids A **1**, 2019 (1989).
[25] R. H. Kraichnan, Phys. Fluids **8**, 575 (1965).
[26] U. Frisch, *Turbulence: The Legacy of A. N. Kolmogorov* (Cambridge University Press, Cambridge, England, 1995).
[27] W. D. McComb, Phys. Rev. E **71**, 037301 (2005).
[28] A. A. Townsend, *The Structure of Turbulent Shear Flow* (Cambridge University Press; Cambridge, England, 1980), 2nd Edition.
[29] J. Counihan, Atmos. Environ. **9**, 871 (1975).
[30] G. D. Nastrom, K. S. Gage, and W. H. Jasperson, Nature (London) **310**, 36 (1984).
[31] S. Lovejoy, D. Schertzer, and J. D. Stanway, Phys. Rev. Lett. **86**, 5200 (2001).
[32] J. F. Muzy, R. Baïle, and P. Poggi, Phys. Rev. E **81**, 056308 (2010).
[33] E. Lindborg, J. Fluid Mech. **388**, 259 (1999).
[34] F. A. Gifford, Agr. Forest Meteorol. **47**, 155 (1989).
[35] C. W. Van Atta and J. C. Wyngaard, J. Fluid Mech. **72**, 673 (1975).
[36] G. I. Taylor, Proc. R. Soc. A **164**, 476 (1938).
[37] J. Mur-Amada and A. Boyad-Rujula, in *Variability of Wind and Wind Power, Wind Power*, edited by S. M. Muyeen (InTech, 2010), ISBN: 978-953-7619-81-7.
[38] M. Wilczek and R. J. A. M. Stevens, Wind Energ., doi:10.1002/we.1929 (2015).
[39] M. Wilczek, R. J. A. M. Stevens, and C. Meneveau, J. Fluid Mech. **769**, R1 (2015).
[40] G. Giebel, (Ph.D. dissertation, Carl von Ossietsky, University of Oldenburg, 2000. Available at: http://www.drgiebel.de/GGiebel_DistributedWindEnergyInEurope.pdf).
[41] R. Steinberger-Willms, Ph.D. dissertation, Oldenburg University, 1993 (Verlag Shaker, Aachen, 1993), ISBN 3-86111-740-1, ISSN 0945-0726.
[42] L. Landberg, M. A. Hansen, K. Vesterager, and Bergstrøm, Report No. Risø-R-929(EN) (Risoe National Laboratory, Roskilde, Denmark, 1997), ISBN 87-5502229-4.
[43] S. Frandsen, J. Wind Eng. Ind. Aerodyn. **39**, 251 (1992).
[44] M. Calaf, C. Meneveau, and J. Meyers, Phys. Fluids **22**, 015110 (2010).
[45] A. L. M. Grant, J. Atmos. Sci. **49**, 226 (1992).
[46] http://www.eirgrid.com/operations/systemperformancedata/windgeneration/.
[47] NOAA National Centers for Environmental Information, https://www.ncdc.noaa.gov.
[48] R. Doherty and M. O'Malley, IEEE Transactions on Power Systems;IEEE Transactions on Power Electronics **20**, 587 (2005).
[49] P. A. Ruiz, C. R. Philbrick, and P. W. Sauer, Pow. Syst. Conf. and Expo. PSCE '09, doi:10.1109/PSCE.2009.4840133 (2009).

Supplemental Material: The Spectrum of Wind Power Fluctuations

M. M. Bandi[1]

[1] *Collective Interactions Unit, OIST Graduate University, Okinawa, Japan 904-0495*[*]

(Dated: December 7, 2016)

Power available in wind

Defining the instantaneous kinetic energy per unit mass in wind with density ρ as $T(t) = (1/2)\rho|\vec{u}(t)|^2 = (1/2)\rho\vec{u}(t)\cdot\vec{u}(t)$, the instantaneous turbulent energy flux or total power available for extraction in wind is given by $\vec{p}(t) \equiv T(t)\vec{u}(t)$. Performing velocity Reynolds decomposition $\vec{u}(t) = \overline{\vec{u}} + \tilde{\vec{u}}(t)$, where $\overline{\vec{u}}$ is the time-independent mean and $\tilde{\vec{u}}(t)$ is the time-dependent fluctuation ($\overline{\tilde{\vec{u}}(t)} \equiv \vec{0}$), and substituting in the instantaneous turbulent power $\vec{p}(t) = \left(\frac{1}{2}\right)\rho(\overline{\vec{u}} + \tilde{\vec{u}}(t))(|\overline{\vec{u}}|^2 + 2\overline{\vec{u}}\cdot\tilde{\vec{u}}(t) + |\tilde{\vec{u}}(t)|^2)$ gives:

$$\begin{aligned}\vec{p}(t) = (1/2)\rho(&\overline{\vec{u}}|\overline{\vec{u}}|^2 + \tilde{\vec{u}}(t)|\overline{\vec{u}}|^2 + 2\overline{\vec{u}}(\overline{\vec{u}}\cdot\tilde{\vec{u}}(t)) \\ &+ 2\tilde{\vec{u}}(t)(\overline{\vec{u}}\cdot\tilde{\vec{u}}(t)) + \overline{\vec{u}}|\tilde{\vec{u}}(t)|^2 + \tilde{\vec{u}}(t)|\tilde{\vec{u}}(t)|^2)\end{aligned} \tag{1}$$

Considering only the streamwise component $P(t)$ of vectorial kinetic energy flux $\vec{p}(t)$ in Eq. 1, past a turbine of cross-sectional area A, and representing it as a scalar valued equation, we have:

$$P(t) = K\left(\overline{u}^3 + 3\overline{u}^2\tilde{u}(t) + 3\overline{u}\tilde{u}(t)^2 + \tilde{u}(t)^3\right) \tag{2}$$

where $K = \left(\frac{1}{2}\right)\rho A\gamma$, and γ is the turbine efficiency.

Power conversion by the turbine

We treat the turbine as a temporal probe of turbulent flow past a fixed (Eulerian) spatial location, much like an anemometer. Whereas both anemometer and turbine are invasive probes, unlike an anemometer whose probe tip is of micrometer (hot wire anemometers) to centimeter dimensions (cup anemometers), a turbine's rotor spans several 10s of meters. Blade Element and Blade Element Momentum theories [1] account for wind speed variations along the blade span by integrating torque along the blade elements. It is customary to then calculate an equivalent wind speed [2] producing the same torque as the non-stationary three dimensional wind field to calculate power fluctuations at the turbine. The equivalent wind speed represents a smoothed (over rotor area A) wind speed time series. Consequently, the turbine does not register short time scale fluctuations from eddies of sizes smaller than rotor diameter. Such short time fluctuations cannot be accounted for in our analysis. The above approach broadly applied by the wind engineering community already effectively treats the rotor as a point (Eulerian) entity.

Our second assumption of adiabatic power conversion, i.e. fluctuations in wind speed are instantaneously converted to power fluctuations, is well placed. Wind speed fluctuations are transmitted to the rotor via pressure variations. Wind power spectra exhibit a spike at very short time scales[3, 4] from pressure difference felt by blades as they pass the turbine mast [5].

Our third assumption is that the turbine extracts same fraction of power at all time scales, i.e. there is no dispersion during power conversion. All turbines have a reaction time scale τ_R due to rotor inertia and associated control system [3]. For timescales $\tau \leq \tau_R$, the turbine applies its own control dynamics and distorts power conversion. This distortion, clearly observed in spectra [3], is a convolution of wind speed dynamics by the control system's filter function. The turbine reaction timescale $\tau_R \sim 1 - 60$ s depends on turbine size and its design among other parameters. It is longer than the fluctuation time scale corresponding to the eddy of rotor area A. The MM92 turbine used in this study had a reaction time scale $\tau_R \simeq 30$ s. Comparison of $S_2^1(\tau)$ and $D_2(\tau)$ in fig. 1b of the main text shows a measurable deviation from $\tau^{2/3}$ scaling for $\tau \leq 30$ s in $D_2(\tau)$, but not in $S_2^1(\tau)$. Our analysis therefore applies only for $\tau > \tau_R = 30s$ and we treat this as the threshold time scale below which our analysis does not hold. This assumption holds approximately for $\tau > \tau_R$. Power conversion occurs primarily due to drag experienced by the turbine blade from wind blowing past it. Whereas Re dependence of drag coefficient is well known, it is weak and may be assumed constant (Re independent) in the range of wind speeds between the turbine's cut-in and rated speeds. The MM92 turbine had a cut-in speed of 3 m/s, rated speed of 11.2 m/s and cut-out speed of 24 m/s.

Finally, we did not have directional fluctuation information for plant (ERCOT) and grid (EIRGRID) scale data. We found no leading order influence of directional fluctuations [6] in the single turbine data; the MM92 turbine yaws in response to directional variations over 10s of seconds $\sim \tau_R$. Whereas a higher order effect should certainly be expected, we did not delve into it in the interests of restricting ourselves to leading order analysis providing a minimal description. Barring this final assumption, all idealised assumptions discussed here concern the validity in treating the turbine as a probe of turbulence, and not the underlying physics leading up to the scalings themselves. As fig. 1 and 2 in the main text attest, the turbine, plant, and grid level data demonstrate robust scalings. Atmospheric flows, particularly

at large scales of up to 100s of km as discussed here, are neither isotropic nor homogeneous. It is noteworthy that K41 and its extensions, which apply to isotropic, homogeneous, and incompressible turbulence, work well for wind power as they have for prior experimental observations of atmospheric turbulence [7].

K41 Dimensional Considerations

In analogy with K41 [8], Ref. [9] considered inertial range scalings for higher order turbulent velocity spectra as functions of $\overline{\varepsilon}$ & r alone, whose calculation in wavenumber domain is presented here in the spatial domain. Consider the difference in longitudinal components of arbitrary powers ($u^m\ \forall\ m \geq 1$) of velocity: $\Delta u^m_{||}(r)$ with $S^m_2(r) \equiv \langle(\Delta u^m_{||}(r))^2\rangle$. Imposing K41 expectation $S^m_2(r) \sim C_m \overline{\varepsilon}^\alpha r^\beta$ ($\overline{\varepsilon}$ has dimensions $[L]^2[T]^{-3}$), we have:

$$\begin{aligned} S^m_2(r) &= C_m \overline{\varepsilon}^\alpha r^\beta \\ [L]^{2m}[T]^{-2m} &= [L]^{(2\alpha+\beta)}[T]^{-3\alpha} \end{aligned} \tag{3}$$

We see $\alpha = \beta = \frac{2m}{3}$. Applying TH to Eq. 3 then yields:

$$S^m_2(\tau) \equiv \langle(\Delta u^m(\tau))^2\rangle = C_m(\overline{u}\overline{\varepsilon}\tau)^{2m/3} \tag{4}$$

Specifically, Eq. 4 gives us $S^1_2(\tau) = C_1(\overline{u}\overline{\varepsilon}\tau)^{2/3}$, $S^2_2(\tau) = C_2(\overline{u}\overline{\varepsilon}\tau)^{4/3}$ & $S^3_2(\tau) = C_3(\overline{u}\overline{\varepsilon}\tau)^2$.

Taylor versus Random Sweeping for $m = 1$

K41 [8] concerns simultaneous velocity measurements made at spatial separations r, whereas wind power concerns temporally separated (over time τ) measurements at the same spatial (Eulerian) location. The two measurements are fundamentally different [10]. Two different situations arise in temporal Eulerian measurements, depending upon the strength of mean speed relative to RMS fluctuations. The uniform sweeping regime where TH applies, arises when $u_{rms}/\overline{u} << 1$; operationally TH applies when $u_{rms}/\overline{u} < 0.1$. Here, the mean speed $\overline{u}$ sweeps all turbulent eddies past the Eulerian probe fast enough, eddies do not evolve over the measurement duration, and one obtains Eq. 4 for $m = 1$:

$$S^1_2(\tau) = C_1(\overline{u}\overline{\varepsilon}\tau)^{2/3} \tag{5}$$

When $u_{rms}/\overline{u} > 0.1$, the effect of eddy evolution during the measurement duration becomes important. A generalization of TH, namely the Random Sweeping Hypothesis (RSH) then applies, which yields:

$$S^1_2(\tau) = C_1(u_{rms}\overline{\varepsilon}\tau)^{2/3} \tag{6}$$

Whereas Galilean invariance is preserved in TH (Eq. 5), it is violated in RSH when u_{rms} replaces $\overline{u}$ in Eq. 6; for details, see Refs. [10–12].

Galilean invariance breakdown for $m > 1$

K41 applies only to Galilean invariant quantities [13, 14] such as velocity differences [15]; RSH being an exception. Since differences in higher powers of velocity ($m > 1$) are not Galilean invariant by default, K41 dimensionality (Eq. 4) no longer applies, irrespective of TH or RSH regimes. Consequently, $S^m_2(\tau) \sim \tau^{2/3}\ \forall\ m > 1$ as we outline for $m = 2$:

$$S^2_2(\tau) = \langle(\tilde{u}(t+\tau) - \tilde{u}(t))^2(\tilde{u}(t+\tau) + \tilde{u}(t))^2\rangle \tag{7a}$$

$$\sim \langle(\tilde{u}(t+\tau) - \tilde{u}(t))^2\rangle\langle(\tilde{u}(t+\tau) + \tilde{u}(t))^2\rangle \tag{7b}$$

$$\sim S^1_2(\tau) 2\langle\tilde{u}^2\rangle(1 + \langle\tilde{u}(t)\tilde{u}(t+\tau)\rangle/\langle\tilde{u}^2\rangle) \tag{7c}$$

$$\sim u^2_{rms} S^1_2(\tau) + \text{ h.o. terms} \tag{7d}$$

In going from Eq. 7a to b, we consider only the leading order term *via* simple decomposition of the statistical average $\langle\ldots\rangle$; for an extensive calculation, see Ref. [7]. In Eq. 7c, $(1+\langle\tilde{u}(t)\tilde{u}(t+\tau)\rangle/\langle\tilde{u}^2\rangle) = 2$, its maximum value, at $\tau = 0$ and $(1 + \langle\tilde{u}(t)\tilde{u}(t+\tau)\rangle/\langle\tilde{u}^2\rangle) \to 1$ as $\tau \to \infty$. The dominant scaling in Eq. 7d follows from $S^1_2(\tau)$ with u_{rms} explicitly entering the scaling. Simple algebraic decomposition $(a^m - b^m) = (a - b)((m-1)$ order term) then always assures $S^m_2(\tau) \sim u^{2(m-1)}_{rms} S^1_2(\tau)$. Simple substitution of Eq. 5 for TH or Eq. 6 for RSH, then yields the scaling form for all $m > 1$:

$$\text{TH}: \ S^m_2(\tau) \sim u^{2(m-1)}_{rms}(\overline{u}\overline{\varepsilon}\tau)^{2/3} \tag{8a}$$

$$\text{RSH}: \ S^m_2(\tau) \sim u^{2(m-1)}_{rms}(u_{rms}\overline{\varepsilon}\tau)^{2/3} \tag{8b}$$

Equation 8 is the temporal counterpart of Eq. 34 in Ref. [7]. The integral scale velocity fluctuation, u_{rms} explicitly enters Eq. 8 as a consequence of the breakdown of Galilean invariance for $m > 1$.

Integral scale of atmospheric turbulence

The streamwise (horizontal) integral scale l_0 varies with vertical height within the atmospheric shear boundary layer [16]. Whereas, historical measurements [17] suggest that at a hub height of 100 m, the integral scale along the streamwise direction is $l_0 \sim 100$ m, our estimate for Howard data $l_0 \sim 200$ km is three orders of magnitude larger. The estimate of $l_0 \sim 200$ km is a consequence of $\tau_0 = 13$ hours, a timescale that accords perfectly with a diurnal forcing of half day. De-trending diurnal oscillation from the time series would certainly shorten τ_0 yielding a smaller value for l_0. However, as a dominant time scale that contains a substantial fraction of the energy, de-trending the diurnal oscillation mode out of the time series seems equally spurious a protocol to adopt. Be that as it may, since Counihan's analysis [17], several new measurements [18–20] strongly attest to the existence of larger coherent length scales spanning several 100 km in atmospheric turbulence.

Surface layer measurements at various locations [20] point to long-range correlations in the atmospheric mesoscale spanning 100s of kilometers. Lovejoy et al [19] have shown the existence of multifractal cascades from planetary scales down to 1 km range from satellite data. Nastrom et al [18] performed aircraft based hot wire anemometry measurements and concluded a two-dimensional turbulence spectrum exhibiting both k^{-3} enstrophy and $k^{-5/3}$ inverse energy cascade regimes. Whereas the spectrum is flipped relative to the regular two dimensional turbulence spectrum as discussed at length by Lindborg [21], the two versus three dimensional character of atmospheric turbulence is not relevant to wind power since turbines of 100 m always experience a full three dimensional flow field. Of particular interest is the fact that the cross-over between k^{-3} and $k^{-5/3}$ occurs at a length scale of order 100 km. Whereas all these recent studies lend strong support to a 200 km integral scale in atmospheric turbulence, the integral scale of atmospheric turbulence is very much an open problem [22]. The most credible proof that concerns the present study comes from direct measurements on wind plants themselves. Results from multiple studies cited in the main text provide incontrovertible evidence of a spatial correlation decay length $\sim$ 100s of kilometers. Based on above arguments, we conclude it is reasonable to assume the inter-plant correlation decay length to be the integral scale of atmospheric turbulence ($D \simeq l_0$).

* Email: bandi@oist.jp

[1] E. Kulunk, *Fundamental and Advanced Topics in Wind Power Ed. R. Carriveau, Chapter 1* (Intech, 2011).

[2] T. Burton, D. Sharpe, N. Jenkins, and E. Bossanyi, *Wind Energy Handbook* (John Wiley & Sons Ltd., England, 2001).

[3] P. Milan, M. Wächter, and J. Peinke, Phys. Rev. Lett. **110**, 138701 (2013).

[4] J. Apt, J. Power Sources. **169**, 369 (2007).

[5] C. V. Moreno, H. A. Duarte, and J. U. Garcia, IEEE Trans. Energy Conv. **17**, 267 (2002).

[6] A. Choukulkar, Y. Pichugina, C. T. M. Clack, R. Calhoun, R. Banta, A. Brewer, and M. Hardesty, Wind Energ. **doi:10.1002/we.1929** (2015).

[7] C. W. Van Atta and J. C. Wyngaard, J. Fluid. Mech. **72**, 673 (1975).

[8] A. N. Kolmogorov, Dokl. Akad. Nauk SSSR **30**, 299 (1941).

[9] D. A. Dutton and D. G. Deaven, *Some properties of atmospheric turbulence. In Statistical Models and Turbulence. Lecture Notes in Physics, vol. 12. Ed. M. Rosenblatt & C. W. Van Atta* (Springer, 1972).

[10] R. H. Kraichnan, Phys. Fluids **7**, 1723 (1964).

[11] H. Tennekes, J. Fluid. Mech. **67**, 561 (1975).

[12] S. Chen and R. H. Kraichnan, Phys. Fluids A.: Fluid Dynamics **1**, 2019 (1989).

[13] R. H. Kraichnan, Phys. Fluids **8**, 575 (1965).

[14] U. Frisch, *Turbulence: The legacy of A. N. Kolmogorov* (Cambridge University Press, UK, 1995).

[15] W. D. McComb, Phys. Rev. E. **71**, 037301 (2005).

[16] A. A. Townsend, *The Structure of Turbulent Shear Flow* (Cambridge University Press; 2nd Edition, 1980).

[17] J. Counihan, Atmos. Environ. **9**, 871 (1975).

[18] G. D. Nastrom, K. S. Gage, and W. H. Jasperson, Nature **310**, 36 (1984).

[19] S. Lovejoy, D. Schertzer, and J. D. Stanway, Phys. Rev. Lett. **86**, 5200 (2001).

[20] J. F. Muzy, R. Baïle, and P. Poggi, Phys. Rev. E. **81**, 056308 (2010).

[21] E. Lindborg, J. Fluid Mech. **388**, 259 (1999).

[22] F. A. Gifford, Agri. Forest. Meteorol **47**, 155 (1989).